Discharge Mechanism in Argon Counters

LAURA COLLI AND UGO FACCHINI
Laboratori C.I.S.E., Milan, Italy
(Received June 30, 1952)

The multiplication curves and the pulse shapes have been studied in a counter filled with pure argon and argon plus carbon dioxide mixtures at pressures ranging from 150 to 1000 mm Hg.

The pulse shapes in argon in the high proportional zone and up to voltages corresponding to the corona threshold are explained by assuming a production in the Townsend avalanche of photons hard enough to extract electrons from the cathode. These photoelectrons are found to be produced during a time Tf_0 of the order of a few μsec when at 150 mm Hg pressure, and during a smaller time when at higher pressures. The analysis of the features of the excited levels of argon suggests the four lower excited levels to be responsible for the photoelectric effect. These photons are produced in collisions leading to destruction of these levels, and are not resonance photons. The Tf_0 values deduced from our measurements are in accordance with those obtained by extrapolating the Molnar values for the first metastable levels at the pressures used. This photoelectric process has been found to be the main one responsible for sustaining corona discharge, which starts at multiplication values of about 200.

If carbon dioxide concentrations varying from 10^{-4} to 5×10^{-3} are added to argon, one obtains an increase of N_S, the threshold multiplication, which is linear *versus* the carbon dioxide percentage. This fact is readily explained by assuming the quenching of argon excited levels by collisions of the second kind on carbon dioxide molecules. From the experimental results one may deduce a value of the quenching cross section which is about 600×10^{-16} cm^2 in a first approximation.

Further studies concern the space charge effect at the photoelectric process divergence threshold, which allows the formation of a very narrow Geiger zone at carbon dioxide concentrations over 5×10^{-4}.

No processes other than the photoelectric one have been found to be efficient in counters filled with argon plus carbon dioxide mixtures up to a concentration of 5×10^{-3}.

At higher percentages the photoelectric process is considerably reduced; there has been found to be effective in the discharge build-up a process by which electrons are released in the gas body. The counter behaves as a regular fast counter.

The effect of mercury vapor in the discharge in pure argon is also described; it is accounted for by the well-known Penning process of mercury ionization by collision on excited argon atoms. This process causes the discharge to start at extremely low multiplication values.

I. INTRODUCTION

THE aim of this work is to inquire into the elementary processes acting in Geiger counters and the building up of pulses in the Geiger zone, in counters filled with very pure argon or argon mixed with carbon dioxide, at concentrations ranging from 10^{-4} to 10^{-1}. Many researches have been carried out up to now to build a theory to account for the behavior and properties of counters.[1,2] These researches have high-lighted some fundamental points on this subject. However, the mechanisms acting in discharge building up are still uncertain, particularly as far as simple gas counters are concerned.

Evidently, a theory explaining the behavior of a counter requires a knowledge of the various processes responsible for the production of electrons, taking into account the gas mixtures and the cathode of the counter used. Researches on these processes in gas discharges have been extensively carried out by many authors; a review on this subject is given by Penning and Druyvesteyn and by Loeb.[3,4] These studies evidence the strong dependence on purity, pressure, and temperature of gas discharge mechanisms. Therefore, it may be said that the results of these measurements are valid only if strictly referred to the particular conditions of work.

[1] S. C. Curran and J. D. Craggs, *Counting Tubes* (Butterworths Scientific Publications, London, 1949).
[2] D. H. Wilkinson, *Ionization Chambers and Counters* (Cambridge University Press, Cambridge, 1950).
[3] M. J. Druyvesteyn and F. M. Penning, Revs. Modern Phys. 12, 87 (1940).
[4] L. Loeb, *Fundamental Processes of Electrical Discharge in Gases* (John Wiley and Sons, Inc., New York, 1939).

II. METHOD OF MEASUREMENT

The experimental method in the present work makes use of the observation of pulses obtained from ionizing particles, in a regular cylindrical counter. Depending on the applied voltage, the counter acts first as an ionization chamber and later as a proportional counter. At a defined voltage value, the counter gets in the corona discharge zone; under suitable conditions, this zone is preceded by a Geiger zone.

Part of our measurements consists of taking the curves which give N, the multiplication factor, as a function of the voltage V; N represents the number of electrons generated on the counter wire in the Townsend avalanche, per primary electron. The primary ionization is obtained by α-particles from a polonium source placed in the counter, or by single fast electrons generated in the counter wall by a γ-ray source outside the counter (in the following called γ-pulses). The multiplication curves are taken by means of α-particles up to N values of about 50. At higher N values, since α-particles cause a distortion in the multiplication factor due to the high charge involved in the avalanche, γ-pulses are used which, under our conditions, give an undistorted multiplication.

Another part of the measurements consists of the study of the shape of pulses in the various zones of voltage of the counter, with different time constants in the amplification chain, in order to obtain pulses variously differentiated. From these observations of the shapes, it is possible to get the discharge development as a function of time, from which one can obtain

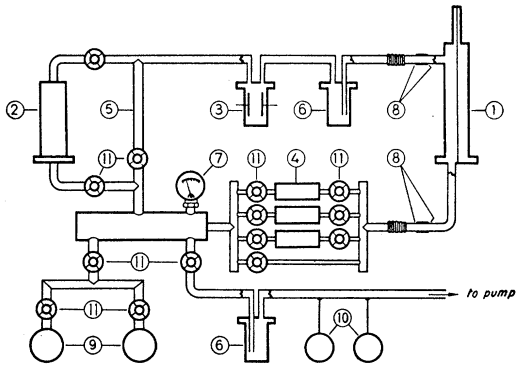

FIG. 1. Experimental apparatus: 1. counter; 2. purification furnace; 3. ionization chamber; 4. reservoirs; 5. heated tube; 6. traps; 7. manometer; 8. Kovar-glass seals; 9. argon and carbon dioxide tanks; 10. vacuum gauges; 11. stopcocks.

information on the nature of processes involved in the discharge and can measure some quantities related to these processes.

III. EXPERIMENTAL EQUIPMENT

The measurements have been taken with different equipment consisting of one or more counters mounted on a manifold suitable for evacuating and filling them with the proper gas mixtures. The apparatus to which most of our data refer is shown in Fig. 1. This consists of a counter inserted in a metal circuit, where the gas will circulate by heating, which provides a fast purification of the argon and a fast mixing of argon plus carbon dioxide mixtures. The counter is of brass; its diameter is 60 mm; the useful length of the tungsten wire is 200 mm and the wire diameter 0.2 mm. The counter can be heated up to 200°C for degassing purposes. The counter tube was degassed at 600°C for a few hours before mounting.

The outstanding elements of the circuit are as follows: (1) The circulation furnace filled with calcium magnesium alloy, with 10 percent magnesium, which provides the argon purification.[5] (2) The ionization chamber which is employed for the measurement of the electron drift-velocity in the gas. This measurement will control the argon purity at 99.99 percent accuracy for molecular impurities.[5] (3) The heated tube, which allows gas circulation even excluding the furnace.

The tight washers and the stopcocks are wholly metallic; in the apparatus there is neither grease nor mercury vapors.

This apparatus in connected to a diffusion vacuum pump, which works with silicone oil. The vacuum is measured by a Penning gauge. The whole apparatus is evacuated for many days at 10^{-5} mm Hg, degassing the counter and the furnace.

The argon employed is from different sources and of initial purity ranging from 98 to 99.9 percent. In every case, the results obtained can be reproduced. The purity of the carbon dioxide was 97 percent.

The counter wire is connected, through a conventional amplification chain, to a cathode-ray tube, Dumont 248 type, the sweep of which is triggered by a

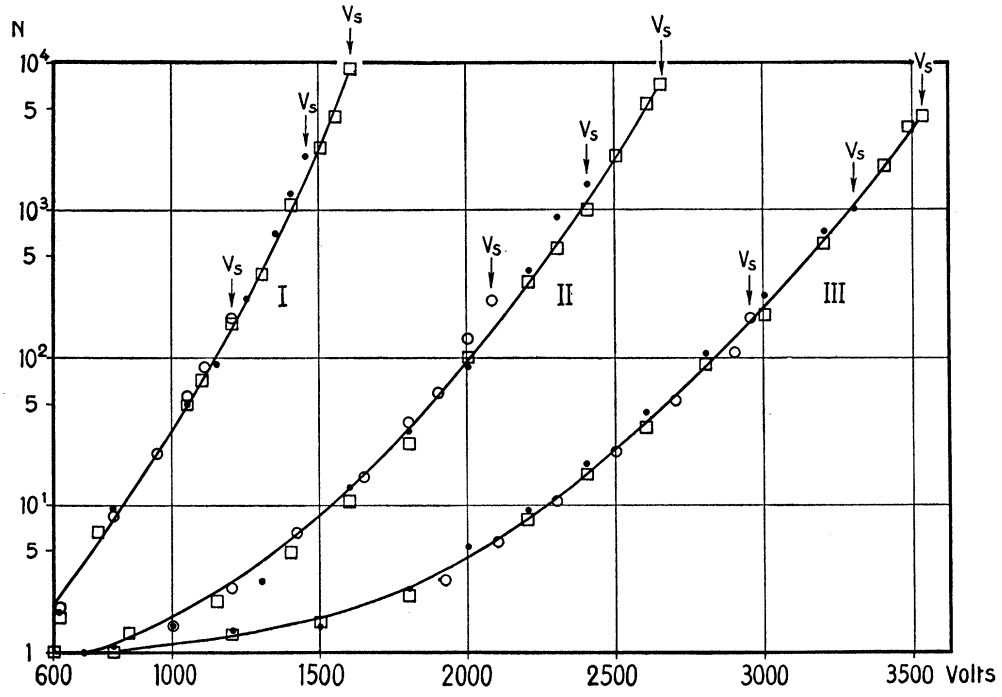

FIG. 2. Multiplication curves for argon and argon+carbon dioxide mixtures. (I) $p=150$ mm Hg; (II) $p=500$ mm Hg; (III) $p=1000$ mm Hg. ○—argon; ●—argon plus 3×10^{-4} carbon dioxide; □—argon plus 17×10^{-4} carbon dioxide.

[5] L. Colli and U. Facchini, Rev. Sci. Instr. 23, 39 (1952).

synchroscope. The rise time of the circuit is 0.6 μsec. In a number of cases it has been found advisable to use a chain with a faster rise time.

The measurements of pulse amplitudes are taken through an input time constant RC much higher than the pulse rise time ($RC=200$ μsec): In this case a pulse shaping delay line is inserted between the preamplifier and the amplifier, which line suppresses the pulse after a time varying from 1.2 to 6 μsec; thus, only the first

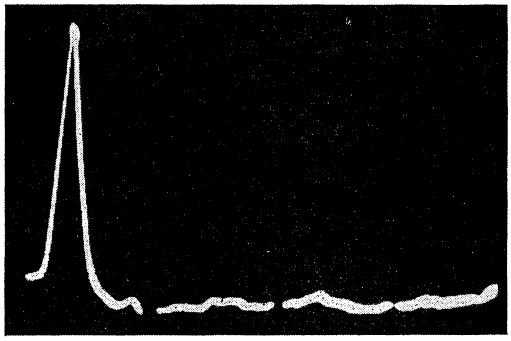

FIG. 3. α-particle pulse in the low proportional zone. Markers=10 μsec; $RC=1$ μsec.

rise of the pulse is recorded, corresponding to the collection of the avalanche electrons, and an eventual component due to a delayed production of electrons is left out. This cut is important in the measurement of the multiplication factor in the highest proportional zone, where these processes of delayed production are considerable.

The pulse shape as a function of time is observed by the synchroscope, using an input time constant varying from 1 to 200 μsec which gives different pulse differentiation. The pulse shape can be observed in a time duration varying from some μsec to about 30 msec using different oscillograph sweep durations.

IV. MEASUREMENT FOR ARGON

The multiplication curves N *versus* V, in argon for pressures ranging from 150 to 1000 mm Hg, are shown in Fig. 2. During the time of measurement the argon circulates in the purification furnace at 400°C (Fig. 1). Under these conditions the measurements are reproducible; no variation has been obtained by placing liquid air round the trap and leaving it there for some hours. The counter is at room temperature.

The α- and γ-pulses observed through the synchroscope are of the usual shape, up to multiplication values of about 50 (Fig. 3). Starting from these multiplication values, each α- or γ-pulse is followed by a convergent succession of pulses separated by a time T_0 (Figs. 4 and 5); the ratio of this succession increases as N increases. The time T_0 between the pulses of the succession is ~10 μsec, at all the pressures studied. These pulses are clearly observed with an RC of 1 μsec, much smaller than their separation.

Observing the pulse succession we can see that the rise time of successive pulses gets longer as the sequence number of the pulse in succession increases (Fig. 5); consequently, the sharpness of the separation between pulses decreases towards the end of the succession. This effect becomes more prominent as the pressure diminishes. At a pressure of 150 mm Hg the second pulse only is detectable, followed by a continuous slope (Figs. 6 and 7).

At a multiplication value of about 200 (Fig. 2), after a few volts of unstable zone the corona discharge starts in the counter. The α-pulse shapes at the beginning of the corona are shown in Figs. 4–7. It should be noted that the successions of pulses are always convergent, as is the case also for γ-pulses.

V. DISCUSSION OF THE RESULTS FOR ARGON

The results obtained for argon, and particularly the pulse shapes at high multiplication, can be accounted for by the processes governing the production and the decay of excited atoms in the Townsend avalanche.

(a) The Photopulses

As is well known, in the proportional zone an electron released in the counter may ionize the argon atoms by collision when it approaches the wire, where the electric field is sufficiently strong, and cause the Townsend avalanche. An electron generated in the counter will thus build up a pulse containing N electrons, the amplitude of which is proportional to N, the multiplication factor.

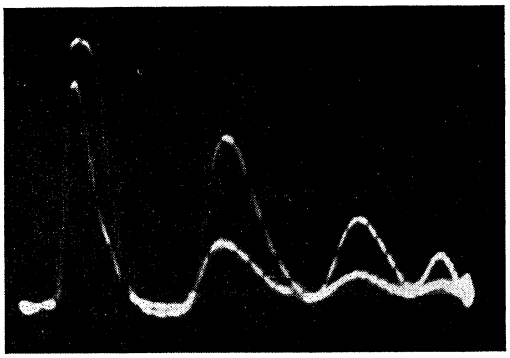

FIG. 4. α-particle pulses in argon at the corona threshold. Pressure =1000 mm Hg; $N=210$; markers=1 μsec; $RC=1$ μsec.

Let us consider now the excited atoms produced in the avalanche; let us call α the ratio between the number of excited atoms and the number of electrons produced by collision in the avalanche. The number of excited atoms produced per initial electron in the gas is $N\alpha$. It can be assumed that the excited levels have a lifetime T_{f0}, and that in the decay processes they generate some photons hard enough to extract electrons from the cathode by photoelectric effect (photoelectric

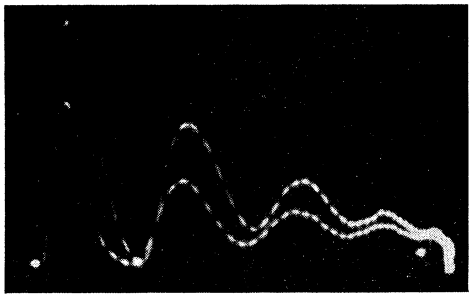

FIG. 5. α-particle pulses in argon at the corona threshold. Pressure = 500 mm Hg; $N = 250$; lengthening of rise time is detectable in the last photopulses; markers = 1 μsec; $RC = 1$ μsec.

threshold of brass 4–5 ev). Let us call β the mean number of "hard" photons emitted per excited atom, G the probability of a photon reaching the cathode without destruction, K the useful solid angle, and γ the mean number of electrons extracted from the cathode and reaching the wire per each photon.

In a time interval of the order of T_{f0}, the $N\alpha\beta$ photons produce $N\alpha\beta GK\gamma$ photoelectrons from the cathode. These photoelectrons reach the wire after a time T_{e0} (transit time in the counter) and multiply by N, giving rise to a second pulse of amplitude proportional to $(N\alpha\beta GK\gamma)\cdot N$ at a time interval about $T_{e0}+T_{f0}$ from the first. This process will repeat, so that a succession of pulses is obtained, the ratio $(N\alpha\beta GK\gamma)$ of which increases as the voltage increases; here we have disregarded the N variation due to the positive charge accumulated on the wire.

At the voltage value where

$$N\alpha\beta GK\gamma = 1, \tag{1}$$

there is the divergence threshold of the process in this approximation. The value of N which satisfies Eq. (1), the threshold multiplication factor, will be called N_S and the corresponding voltage V_S.

The pulse succession described in Sec. IV, the behavior as a function of voltage, and the starting of corona discharge can be explained by this process. The single photopulses of the succession can be observed properly separated only if the time T_{f0} is much lower than T_{e0}. If T_{f0} is not negligible compared to T_{e0}, the pulse rise times are obviously lengthened; therefore, their separation is worse.

The photographs of pulse successions show that pulse rise times get longer for the last pulses of the succession; this lengthening becomes more important as pressure decreases until, at lowest pressures, the photopulses are no more separated. These facts appear to indicate that the time T_{f0} increases as pressure decreases. A cause of lengthening of the rise times in the next pulses might be due to an action of the developing time of the electronic avalanche and also to a geometrical diffusion of the pulses along the counter. We may assume these effects to be negligible, since in A+CO_2 mixtures (see Sec. VII) several tens of well separate photopulses and no considerable lengthening of the rise times can be observed. Under these conditions, geometrical or avalanche actions will occur in a way similar to that which occurs in pure argon, without causing any considerable effect. Some information on the T_{f0} value can be obtained by measuring T_0, the distance between the maxima of the two first pulses, and calculating T_{f0} from the relation $T_{f0}+T_{e0}\simeq T_0$.

FIG. 7. α-particle pulse in argon at the corona threshold. Pressure = 150 mm Hg; $N = 180$; sweep time = 100 μsec; $RC = 10$ μsec.

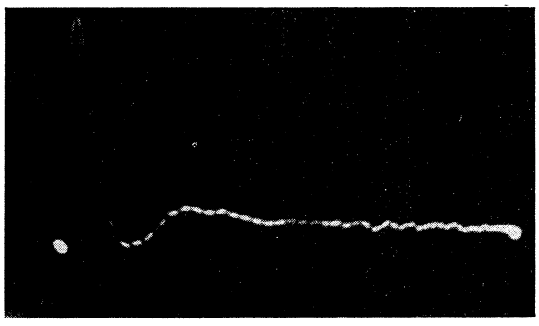

FIG. 6. α-particle pulse in argon at the corona threshold. Pressure = 150 mm Hg; $N = 180$; markers = 1 μsec; $RC = 1$ μsec.

T_{e0} is calculated with sufficiently high accuracy by the drift-velocity values w^- of electrons *versus* E/p.[5] These drift-velocity values have been controlled in the same apparatus by the chamber shown in Fig. 1. Nielsen's values for w^- have been employed for E/p higher than 1.5 volt cm^{-1} mm Hg^{-1}.[6]

Values for T_0, T_{e0}, and $T_0-T_{e0}\simeq T_{f0}$ are shown in Table I. These values are to be looked on only as orders of magnitude of the lifetime of excited levels in the gas; in the case of high pressures the values obtained are actually only upper limits. The assumption of a decay time T_{f0}, of the order of magnitude shown in the table, accounts for the pulse shape and gives a simple explanation of the results obtained for the argon plus carbon dioxide mixtures, as will be seen later.

[6] R. A. Nielsen, Phys. Rev. **50**, 950 (1936).

(b) The Decay of the Excited Levels

We now analyze more particularly the decay phenomena of excited levels in the avalanche, in order to make clear the meaning of the time T_{f0} and to discuss its order of magnitude.

In view of this, let us consider the level spectrum of argon as shown in Table II.[7,8] Among the four lower excited levels, the $^3P_1$ and $^1P_1$ are radiant resonance levels, the $^3P_2$ and $^3P_0$ are metastable levels. All these levels have a certain lifetime in the gas, as will be shown below.[9] Among the upper levels, only a few may decay directly to the fundamental level, sending out photons of 14–15 ev; most of these levels will decay, through successive steps or directly, to one of the four lower levels, releasing photons of energy less than 4 ev at all times. The lifetime for these transitions is generally of the order of 10^{-7}–10^{-9} sec, much smaller than the lifetime of the four lower levels.

It should be pointed out that the photons created in these transitions are too soft to produce photoelectric extraction from the cathode; therefore, no further mention of them will be made. Under these conditions, it appears that in any initial distribution of the excitation, after a time corresponding to a few radiant transitions, resonance and metastable levels only are present in the gas.

The $^3P_1$ and $^1P_1$ levels will decay at the fundamental state giving out resonance photons of 11.62 and 11.82 ev. The resonance photons, as is well known, will undergo a diffusion process through which they are captured and re-emitted many times by the nonexcited atoms in the gas. Holstein[10] developed a theory of this process; he calculates that the imprisonment factor $1/g$ (number of captures and re-emissions for a photon, before reaching the containing walls) for a cylinder a few centimeters in diameter is of the order of a few hundreds. According to this theory, the imprisonment duration in our case may be of about 10^{-4}–10^{-5} sec. Holstein deduces also that the imprisonment factor $1/g$ is independent of pressure in a pressure range where the shape of the emission line is determined by the pressure broadening. Experimental measurements giving a value for $1/g$ in argon are not available.

TABLE I. Values of the decay time T_{f0} in argon.

Pressure (mm Hg)	V_S volts	T_0 (μsec)	T_{e0} (μsec)	$T_{f0}=T_0-T_{e0}$ (μsec)	$(T_{f0})_M$ (μsec)
150	1200	10.8±1	6.3±1	4.5±2	4.1
300	1640	10.7±1	7.1±1	3.6±2	1.1
500	2070	10.2±1	7.7±1	<2.5	0.4
1000	3000	10.5±1	8.8±1	<1.7	0.1

TABLE II. Excited levels of argon atom.

Term	Excitation energy ev	Remarks
$^1S_0$	0	Fundamental state
$^3P_2$	11.545	Metastable level
$^3P_1$	11.620	Resonance level
$^3P_0$	11.720	Metastable level
$^1P_1$	11.825	Resonance level
$^{1,3}S, P, D$	12.7–13.3	
$^{1,3}P$	14.0–14.9	
$^{1,3}P, D, F$	14.1–14.3	
	15.68 15.86	Ionization

Metastable levels have very long lifetimes of their own; the process causing their decay is collision with nonexcited atoms of the gas. The lifetime of the $^3P_2$ metastable level in argon has been recently investigated by Molnar[11,12] and Phelps,[13] at pressures from 1 to 10 mm Hg. From these measurements the metastable lifetime was found to be of the order of some msec, and the probability of destruction of metastables in the gas was found to be proportional to the square of the pressure.

According to these authors, the metastable destruction can be accounted for by some collision between metastable and unexcited atoms, leading to the formation of unstable excited molecules which will rapidly decay. There is good reason to assume that hard photons are produced by this process; these photons, being nonresonance ones, will reach the cathode without capture by gas atoms.

Many other phenomena of the gas discharge were interpreted through processes of this kind;[14] however, evidence of their existence is available at present only in the mercury[15] and helium[16] cases.

A suitable theory of the decay of metastable and resonance levels has not been developed up to now, and the experimental data are rather insufficient; furthermore, the decay is complicated by collision processes which, owing to the small energy difference among the first excited levels of argon, of the order of the thermal energy, may lead to transitions between them.

However, the following remarks can be made: At high pressures, the decay of all the first levels can be considered as a whole, taking into account the transitions by collisions. Two possibilities exist: (1) The levels decay through the emission of resonance photons reaching the cathode, with a probability per second almost independent of pressure, represented by g/τ^*, where τ^* is the radiant lifetime of resonance levels. (2) They decay through the process described by Molnar, the probability of which increases with the

[7] W. de Groot and F. M. Penning, *Handbuch der Physik* (J. Springer, Berlin, 1933), 23/1.
[8] C. E. Moore, *Atomic Energy Levels*, National Bureau of Standards Circular No. 4467 (1949).
[9] A. C. G. Mitchell and M. W. Zemansky, *Resonance Radiations and Excited Atoms* (MacMillan Company, New York, 1934).
[10] T. Holstein, Phys. Rev. **72**, 1212 (1947); **83**, 1159 (1951).
[11] J. P. Molnar, Phys. Rev. **83**, 933, 940 (1951).
[12] J. P. Molnar, private communication.
[13] A. V. Phelps, Phys. Rev. **82**, 567 (1951).
[14] E. W. Pike, Phys. Rev. **53**, 921 (1938).
[15] A. Q. McCoubrey, Phys. Rev. **84**, 107 (1952).
[16] R. Meyerott, Phys. Rev. **70**, 670 (1946).

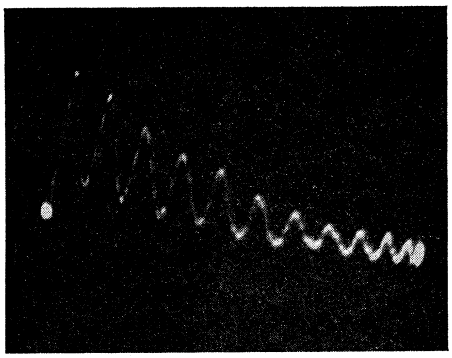

FIG. 8. β-pulse in argon plus 5×10^{-4} carbon dioxide near the Geiger threshold. Pressure = 500 mm Hg; markers = 1 μsec; $RC=1$ μsec.

square of pressure. This process is likely to become more and more important at higher pressure, finally controlling completely the decay of all levels. As a result, the resonance photons practically do not reach the cathode and the photoelectric effect is caused by the photons originated in the collisions of the type described by Molnar. From the description given above β and γ should be referred to these photons and G is thought to be 1. Following these considerations we extrapolated Molnar's results, obtaining the values $(T_{f0})_M$ listed in Table I. These values are of the same order of those obtained by our measurements. Consequently our results give further evidence of the existence of a process causing fast destruction of the afore-mentioned levels in the argon at high pressure.

The decay processes will be further discussed in a subsequent paper.[17]

(c) The Corona Threshold

We now consider the pulse shapes at the corona threshold. If the corona discharge is sustained by the photoelectric process only, the corona threshold is reached when N, the multiplication factor, satisfies Eq. (1); $N\alpha\beta K\gamma$ represents the ratio of the pulse succession which, in this case, should have all the terms constant. When observed with a RC of 1 μsec the shape of the pulse succession from γ-pulses at the corona threshold is always convergent.

The small RC values used may produce a decrease in the ratio of the succession because of the fact that the pulse rise times will increase towards the end of the succession. Roughly considering this electronic distortion, the ratio of the succession at the corona threshold may be evaluated as no less than 0.7–0.9.

Under these conditions, a contribution to the corona discharge from some other processes cannot be completely disregarded. Such processes might be made undetectable in the pulse shape by the experimental conditions of the observation. It can be said, however, that processes other than the photoelectric effect do not contribute in a large measure to the corona discharge considerably at our gas pressures and with our brass cathode.[18]

[17] To be published in *Nuovo Cimento*.

VI. ARGON PLUS CARBON DIOXIDE MIXTURES—PHOTON QUENCHING

Argon plus carbon dioxide mixtures have been studied in the apparatus described under III, at pressure ranging from 150 to 1000 mm Hg. The results obtained with concentrations lower than 5×10^{-3} are reported here.

(a) Experimental Results

Multiplication curves and pulse shapes have been observed for different voltages and for different mixture concentrations. Figure 2 shows a number of these multiplication curves. The curves corresponding to the same pressure have a common part where they are coincident within the experimental accuracy, of the order of 20 percent.

The pulse shapes show that at high multiplication values, each ionizing particle gives rise to a pulse succession of the same kind as described for pure argon (Figs. 8 and 9). The ratio of the pulse succession increases with the multiplication factor as usual until the divergence is reached. In these mixtures a value for this ratio of 1 or over 1 has been observed without a stable corona discharge in the counter.

A detailed discussion of the behavior of the counter at the divergence threshold will be given in Sec. VII.

We are now interested in the study of N_S, the multiplication factor at the divergence threshold (by divergence threshold is meant the voltage value V_S where the ratio of the pulse succession is 1). N_S values obtained *versus* the carbon dioxide percentage X at various pressures are shown in Fig. 10. N_S is shown to increase almost linearly with X, and the slope of the straight lines $N_S(X)$ is found to be steeper for low values of pressure.

(b) Discussion

From the fact that in the proportional zone the same N value corresponds to the same voltage for different carbon dioxide concentrations, we can deduce that the structure of the Townsend avalanche does not depend on small carbon dioxide concentrations. As a consequence, the number α of excited atoms produced in

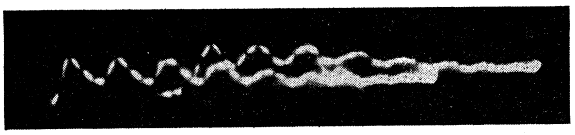

FIG. 9. β-pulses in argon plus 17×10^{-4} carbon dioxide around the Geiger threshold. Pressure = 150 mm Hg; markers = 1 μsec; $RC=1$ μsec.

[18] We note that recently E. J. Lauer (J. Appl. Phys. **23**, 300 1952) has brought in view the presence of a process of ion cathode extraction in argon, using degassed nickel cathodes.

the avalanche per electron may be assumed to be independent of X.

The pulse successions observed in all mixtures hereto discussed may be interpreted as being caused by the photoelectric effect; the ratio of the succession is given by $N\alpha\beta\gamma KG(1-P)$, which will increase with the voltage. P stands for the probability of destruction of excited atoms of argon through collisions with carbon dioxide molecules, without sending out photons efficient in photoelectric extraction.

The threshold value N_S is determined by

$$N_S=1/[\alpha\beta\gamma KG(1-P)]. \quad (2)$$

The quantities involved generally depend on pressure and carbon dioxide concentration.

It is not definitely known if γ, photoelectric yield of the cathode, depends on X. We consider γ to be roughly independent of X; α, β, and K have to be considered constant. The strong variation of N_S as a function of X may therefore be attributed either to the reduction of G, the probability of the photons reaching the cathode, or to an increase of P. We shall now analyze these two cases. G could be reduced by absorption of photons by carbon dioxide. It may readily be seen that this process should produce an exponential dependence of N_S on the total amount of carbon dioxide contained in the counter. The experimental results disagree with this conclusion, the dependence of N_S on X being linear and the dependence of N_S on total pressure going in the opposite direction to that expected. This, as a consequence, will exclude photon absorption as the main process controlling the N_S reduction. We can say that $G=1$ even for the mixtures discussed here.

TABLE III. Values of $\bar{\sigma}T_{f_0}$ and of $\bar{\sigma}$ deduced from the curves of Fig. 10.

Pressure (mm Hg)	$n_A\bar{V}\bar{\sigma}T_{f_0}$	$n_A\bar{V}$ cm^{-2} sec^{-1}	$\bar{\sigma}T_{f_0}$ cm^2 sec	$\bar{\sigma}$ cm^2
150	33,820	0.18×10^{24}	187.8×10^{-21}	458×10^{-16}
500	14,507	0.61×10^{24}	23.8×10^{-21}	595×10^{-16}
1000	7720	1.22×10^{24}	6.33×10^{-21}	633×10^{-16}

Let us now consider the P variation. In this case the collisions of the second kind between excited argon atoms and carbon dioxide molecules have to be taken into account.[9] The excitation energy of the atom is generally transferred to the molecules concerned, which may dissociate or be excited or ionized. In the case under consideration, the most probable reaction is as follows[19]:

$$CO_2+A^*\rightarrow CO^*+O+A+5.5 \text{ ev}.$$

The carbon monoxide molecule is left excited with 6 ev. The reaction energy is thus 11.5 ev, very close to the energy of the excited metastable and resonance levels of argon. This fact increases the probability of the process in question because of resonance.[20]

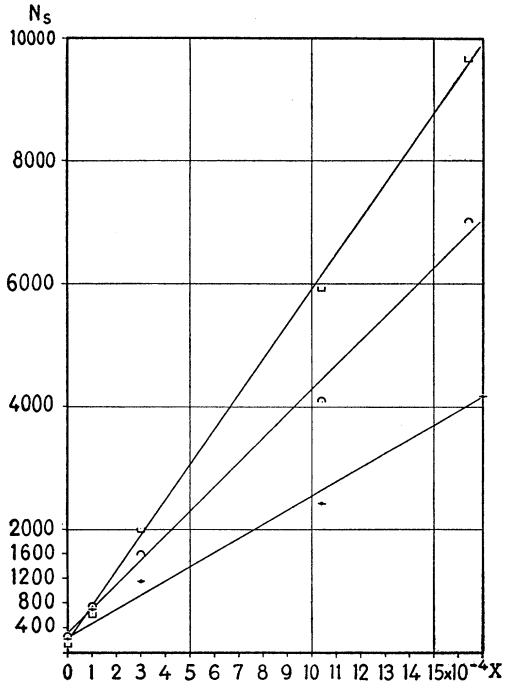

FIG. 10. Values of N_S *versus* CO_2 concentration X. The half-squares are for a pressure of 150 mm Hg; the half-circles are for a pressure of 500 mm Hg; and the bars are for a pressure of 1000 mm Hg.

In a first approximation, let us consider the excited atoms existing in an excited level only, and let N^* be their number in the counter. Under this hypothesis, the equation representing the decay of such atoms is

$$dN^*=-(N^*/T_{f_0})dt-N^*n_AX\bar{\sigma}\bar{V}dt, \quad (3)$$

where T_{f_0} in the lifetime of the level in pure argon. $-N^*/T_{f_0}$ represents the exponential decay accounting for the destruction in argon. $-N^*n_AX\bar{\sigma}\bar{V}$ represents the destruction of excited levels by collisions on carbon dioxide molecules. n_AX is the number of carbon dioxide molecule per cm^3, n_A the number of argon atoms per cm^3, $\bar{\sigma}$ the mean cross section for the quenching process in carbon dioxide, and $\bar{V}$ the mean velocity of atoms.

The fraction of excited atoms destroyed in argon with production of the useful photons is given by

$$1-P=1/[1+n_A\bar{V}\bar{\sigma}T_{f_0}X]. \quad (4)$$

From Eqs. (2) and (4) and assuming $G=1$, we have

$$N_S=(1+n_A\bar{V}\bar{\sigma}T_{f_0}X)/(\alpha\beta\gamma K). \quad (5)$$

In this approximation the formula (5) indicates N_S to be a linear function of X. This formula is satisfactorily verified by the experimental results, considering the errors of the measurements.

[19] H. J. Henning, Ann. Physik **13**, 529 (1932).

[20] N. F. Mott and H. S. Massey, *The Theory of Atomic Collision* (Oxford University Press, London, 1949), Chapter XII.

FIG. 11. β-pulses in the Geiger zone. Argon plus $\sim 10^{-3}$ carbon dioxide; pressure=760 mm Hg; sweep time=50 μsec; $RC=1$ μsec.

From Eq. (5) and the results in Fig. 10, the $T_{f_0\bar{\sigma}}$ values can be obtained for various pressures, the other parameters being known. The values obtained, listed in Table III, decrease as the pressure increases, following a law proportional to the square of pressure. This result is in accordance with the law of destruction found by Molnar in pure argon for the metastable level. The $\bar{\sigma}$-values listed in the last column of Table III have been calculated with the aid of the $(T_{f_0})_M$ values, obtained by extrapolating Molnar's values (Table I).

Some information on the behavior of the resonance and metastable levels due to the different values for the quenching cross section and to the transition probabilities between them, may be obtained by studying the quenching curves to closer approximation, particularly the lower part where most of the excited atoms are destroyed. The poor accuracy of our measurements and the lack of information now available on these processes do not allow us to improve our own results. Therefore, the exact meaning of $\bar{\sigma}$ shown in Table III is uncertain too.

(c) Argon Purity

From Fig. 10, the N_S values appear to be influenced by carbon dioxide concentrations of the order of 10^{-4}. From this we can deduce that the argon used for mixtures contains less than 10^{-4} carbon dioxide or other impurities having the same quenching effect.

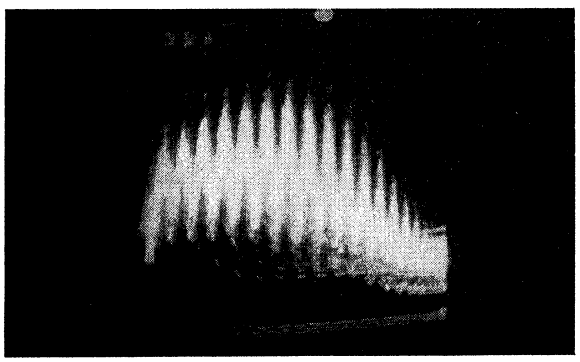

FIG. 12. Several superposed β-pulses in the Geiger zone. Argon plus 1.7 10^{-3} carbon dioxide; pressure=1000 mm Hg; distance between photopulses=4.4 μsec; $RC=1$ μsec.

VII. ARGON PLUS CARBON DIOXIDE MIXTURES—GEIGER ZONE FORMATION

(a) Experimental Results

We consider here the pulse shapes observed in the case of argon plus carbon dioxide mixtures with carbon dioxide concentrations less than 5×10^{-3}, and particularly the pulse shapes at the divergence threshold of the photoelectric process.

(1) *Pulse Shapes*

As stated in Sec. VI, the α- or γ-pulses at high multiplication values consist of photoelectric pulse successions, whose ratio increases with the voltage. Examining the pulses obtained at pressure of 150, 500, 1000 mm Hg and with mixtures containing various carbon dioxide concentrations, the following results are obtained:

(1) The time distance T between the successive pulses of the succession decreases as the carbon dioxide percentage increases. The values of T obtained under the said conditions are shown in Table IV.

TABLE IV. Values of the total time T, between photopulses, in argon and argon+carbon dioxide mixtures.

Pressure (mm Hg)	CO_2 concentration	T (μsec)
1000	0	10.5
1000	10^{-4}	8.9
1000	3×10^{-4}	8.1
1000	9×10^{-4}	6.3
1000	17×10^{-4}	4.4
500	0	10.2
500	10^{-4}	8.3
500	3×10^{-4}	7
500	9×10^{-4}	6
500	17×10^{-4}	4.1

(2) The sharpness of the pulse separation will improve as the carbon dioxide percentage is increased. At 5×10^{-4} carbon dioxide concentrations and 500–1000 mm Hg pressure, some hundred pulses are clearly observable in a γ-pulse succession. Under these conditions, no lengthening of pulse rise times is observed. At 150 mm Hg pressure, the photopulses are well separated only at carbon dioxide concentrations higher than 10^{-3} (Fig. 9).

(2) *Divergence Corona Threshold; Mixtures with Carbon Dioxide Concentrations less than 5×10^{-4}*

In these mixtures, as the multiplication value N_S corresponding to the divergence threshold is reached, the unstable corona discharge will start abruptly. The γ-pulses at this corona threshold consist of a very long pulse succession, containing even some hundred pulses. The succession will first go on with ratio a little lower than 1 and later with ratio about 1. Each γ-pulse may be considered as a corona burst, statistically quenched. This unstable corona zone lasts for only a few volts, after which the corona discharge is stable.

(3) Geiger Zone Formation: Mixtures with Carbon Dioxide Concentrations Ranging from 5×10^{-4} to 5×10^{-3}

With these concentrations, the multiplication factor N may reach values above N_S without the corona discharge getting started in a zone of voltage of very small amplitude, a few tens of volts. In this zone a particle gives rise to a pulse of the kind shown in Fig. 11. The pulse succession will go on first with divergent terms, afterwards with convergent terms until it is exhausted. The structure of these pulse groups does not depend on the primary ionization (Fig. 12). For this reason this photopulse group may be called a Geiger pulse group, and the divergence threshold V_S corresponds to the Geiger zone threshold.

The Geiger zone is followed by the unstable corona zone, lasting a few volts, where the pulse groups are statistically quenched. Figure 13 represents the corona bursts where the photoelectric pulse structure is revealed by an RC of 1 μsec. The amplitude of single photopulses oscillates periodically.

At the end of this zone the coron discharge gets stable with oscillating amplitude.

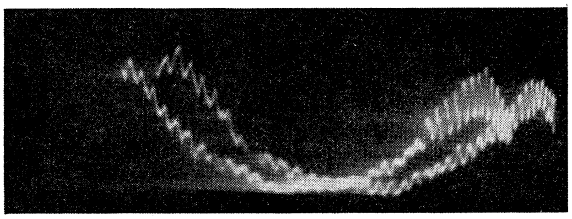

FIG. 13. Detailed bursts in unstable corona zone. Argon plus $\sim10^{-3}$ carbon dioxide; pressure=760 mm Hg; sweep time=100 μsec; $RC=1$ μsec.

A behavior of this kind has been observed in many other counters 2 to 15 cm in diameter, at pressure ranging from 200 to 1500 mm Hg and filling mixtures of argon plus 0.1 percent carbon dioxide.[21] Complete corona bursts for these counters are shown in Figs. 14 and 15, which are taken with a high time constant.

(a) Discussion

(1) Time Distance between Photopulses

As discussed in Sec. V, the time distance T between the photoelectric pulses is the sum of the two times T_f and T_e; T_f is the decay time of the excited levels in the mixture and T_e the transit time of photoelectrons through the counter. From the considerations given in Sec. VII, it can be deduced that T_f is strongly reduced due to the effect of quenching of argon excited levels by carbon dioxide;[22] T_e is also reduced because of the carbon dioxide effect of increasing the electron drift-velocity.[23] The carbon dioxide percentage of 0.1 percent increases the drift-velocity in argon by a factor of two.[5]

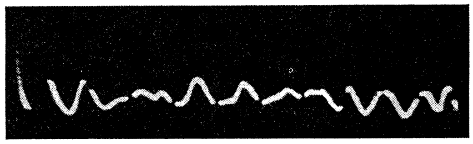

FIG. 14. Burst at the end of unstable corona zone. Argon plus $\sim10^{-3}$ carbon dioxide; counter diameter=20 mm; pressure=760 mm Hg; markers=100 μsec; $RC=10$ μsec; The photoelectric pulse groups appear like single pulses, due to the high RC value.

By the strong quenching effect shown in the curves of Fig. 10, T_f is found to be reduced more considerably than T_e. This agrees with the fact that the sharpness of the separation between the photopulse gets better as the carbon dioxide percentage increases.

(2) Space Charge Effect

The pulse shapes at the beginning of the corona discharge at various mixture concentrations and the Geiger zone formation are readily explained by considering the effect of the space charge accumulated on the wire. In the pulse succession, the delayed photoelectrons reaching the wire are affected in their multiplication process by the space charge formed in the preceding avalanches. Because of that, the multiplication factor N of the successive avalanches will be reduced.

The calculation of pulse build-up taking into account all the successions and the spreading of the pulse along the wire has not been attempted because of its difficulty; nevertheless, it is easily shown that the reduction of the multiplication factor is higher as the process of avalanche regeneration is faster and as the positive ion density is higher. This density is directly proportional to the multiplication factor, at the threshold N_S. Since the T values decrease and the N_S values increase as the carbon dioxide concentration increases, there is good reason to believe that the reduction effect on the succession ratio due to space charge is stronger at higher concentrations. Particularly, at concentrations higher than 5×10^{-4} ($T<7$ μsec, $N_S>2000$) this effect prevents the corona discharge from beginning at N_S

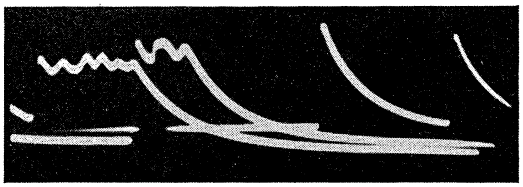

FIG. 15. Bursts in unstable corona zone. Argon plus $\sim10^{-3}$ carbon dioxide; counter diameter=130 mm; pressure=760 mm Hg; sweep time=30 msec; $RC=200$ μsec.

[21] Colli, Facchini, and Gatti, Phys. Rev. **80**, 92 (1950); **84**, 606 (1951).

[22] T_f is related to N_S and T_{f0} by the formula $T_f=(T_{f0}/N_S)\cdot(1/\alpha\beta\gamma K)$.

[23] B. Rossi and H. Staub, *Ionization Chambers and Counters* (McGraw-Hill Book Company, Inc., New York, 1949).

FIG. 16. Geiger pulse in the middle Geiger zone. Argon plus 10^{-2} carbon dioxide; pressure=500 mm Hg; markers=1 μsec; RC=1 μsec. The discharge spreading is due to both the photoelectric effect and a production of electrons in the gas.

and produces self-quenching of pulses, even though they have an initial ratio higher than 1.

The pulse shape shown in Figs. 11 and 12 may be explained as follows. Initially, the multiplication factor N is higher than N_S and consequently the succession proceeds at increasing terms. The positive space charge accumulated on the wire by the first pulses reduces the electric field so that N is brought below N_S; this occurs at the maximum photopulse of the succession. After this, N is kept below N_S until the whole succession is exhausted. By means of this mechanism, the discharge is spread along the whole counter wire.

The Geiger zone formation is clearly due to the space charge effect, which conclusion is in agreement with many authors.[1,24] From our observations, however, this occurs only at carbon dioxide concentrations higher than 5×10^{-4}.

The shapes of the corona bursts shown in Figs. 13, 14, and 15 are explained by the formation and the migration of positive ions, causing the field on the wire to oscillate about the threshold value. Evidently, N has the value N_S at the maxima and minima of the succession. Under these conditions, the space charge is no more able to quench the pulse succession.

(3) *Geiger Zone—Slow Counters*

As said above, the Geiger zones are very small and therefore cannot be used as counting zones. It may be noted, however, that they are observed with small time constant values (from 1 to 200 μsec) and without an external quenching circuit. Obviously, by using higher RC values or a quenching circuit, better Geiger zones could be obtained.

The behavior of these counters is of the same kind as that of the so-called slow counters.

(4) *Other Processes*

The sharpness of the photopulse separation and their time correlation up to several milliseconds indicate that other processes play a role negligible in comparison with the photoelectric process on the cathode, which process entirely explains the Geiger and corona zones. Particularly, a production of electrons in the gas is not important at the pressures and concentrations studied.

The electron extraction from the cathode by ion impact was not found to be efficient in our counters. This process should produce electrons after a time interval from the first avalanche corresponding to the ion transit time in the counter, which ranges from 2 to 8 msec, approximately, in the various conditions. Further, in the argon plus carbon dioxide mixtures, at concentrations between 5×10^{-4} and 5×10^{-3} where the Geiger zone is present, we have the following evidence against the ion-cathode process:

(1) The end of the Geiger zone is determined by the photoelectric process itself.

(2) In the corona bursts the single photopulses are clearly observable and correlated up to times corresponding to the ion transit time. A prominent electron production is not detectable here.

(3) The maxima of the corona bursts occur at a time smaller than the ion transit time.

(4) In the Geiger zone self-quenching separated pulses are observed. The total charge contained in a Geiger pulse is $\sim10^8$ electron charges. From this it can be deduced that the ion-cathode process yield is less than 10^{-8}.

VIII. ARGON PLUS CARBON DIOXIDE MIXTURES—FAST COUNTERS

In the case of mixtures with carbon dioxide percentage higher than 0.5 percent only a few observations have been made.

At pressures of 500 and 1000 mm Hg and 1 percent carbon dioxide percentage the photoelectric process will act at high multiplication values. The time interval between photopulses is about 2 μsec and the N_S value is about 20,000–40,000; here we have the beginning of the Geiger zone, which lasts a few hundred volts. In the first part of the Geiger zone the pulse shape is like Fig. 12 and its amplitude increases with voltage. Fur-

FIG. 17. Several superposed fast pulses at the end of the Geiger zone. Argon plus 10^{-2} carbon dioxide; pressure=500 mm Hg; markers=1 μsec; RC=1 μsec. The discharge will spread solely by the process producing electrons in the gas body.

[24] C. G. Montgomery and D. D. Montgomery, Phys. Rev. **57**, 1034 (1940).

thermore, as the voltage increases the sharpness of the separation between photopulses gets worse until the Geiger pulse looks like Figs. 16 and 17. At 150 mm Hg pressure, the Geiger zone begins at an N_S value of about 80,000 and the Geiger pulses already at the threshold look less discontinuous as in Fig. 16.

With 10 percent carbon dioxide percentage, at the Geiger threshold, the pulses immediately take the continuous shapes shown in Fig. 17 at all pressures used, and there are no photoelectric pulses. Because of this, the threshold multiplication factor is difficult to measure.

The Geiger zone and the pulse shapes described above are of the kind obtained in the case of argon plus organic vapor mixtures.

The continuous shapes and the short durations of the observed Geiger pulses suggests a process of secondary electron production in the gas which is in accordance with the present knowledge on the discharge spreading mechanism in fast counters.[25] The high speed of the process both at the cathode and in the gas makes the quenching effect of the space charge very efficient and allows the formation of longer Geiger zones.

At the Geiger zone end, there are multiple pulses as in the argon plus alcohol counters. The corona discharge is started by these multiple pulses. The nature of these pulses has been investigated by many authors. However, the processes responsible of their formation are not known definitely at present.[26]

IX. ARGON PLUS MERCURY VAPOR MIXTURES

This section deals with the results obtained in argon contaminated with mercury vapor at 1.2×10^{-3} mm Hg pressure, corresponding to room temperature. This study has been carried out in an apparatus similar to that described under Sec. III.

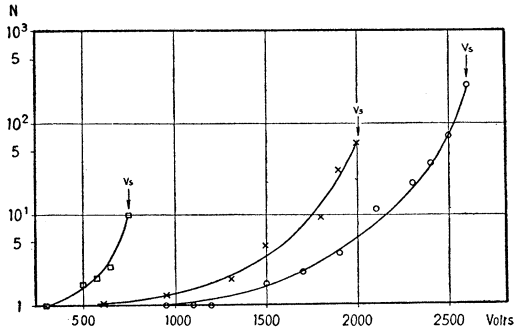

FIG. 18. Multiplication curves for argon plus mercury mixtures. Mercury at 20°C vapor pressure; □—pressure=200 mm Hg; ×—pressure=600 mm Hg; ○—pressure=900 mm Hg.

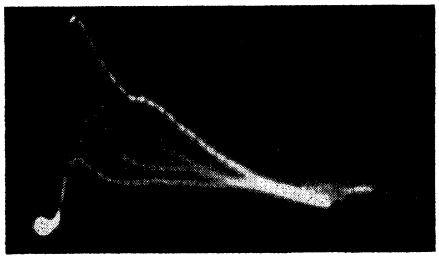

FIG. 19. α-particle pulses in argon plus mercury vapor at the corona threshold. Pressure=1000 mm Hg; markers=1 μsec; RC=1 μsec. The slow decay is due to production of electrons in the gas.

The multiplication curves for three pressures are shown in Fig. 18. At the V_S values the corona discharge will abruptly start. The corresponding N_S values are much smaller than for pure argon without mercury vapor.

At low pressures (200–500 mm Hg) no photopulse is detectable in the pulse shapes at the corona threshold, when observed by a 1 μsec time constant. The pulse shape at 1000 mm Hg pressure is shown in Fig. 19. Here the bump superposed on the continuous slope is due to the photoelectric effect on the cathode. The continuous slope drops more slowly than the time constant of the electronic circuit.

The results may be easily explained by the discussion of Secs. V and VI, after taking into account the Penning effect[7]; this effect is the ionization of mercury atoms by collision on the argon excited atoms. The ionization energy of mercury, 10.4 ev, is lower than the excitation energy of the first four argon levels. During their lifetime in the gas, the excited atoms may ionize by collision the mercury atoms; the free electrons created by this process will start the discharge again.

Our results in argon plus mercury vapor show that at low pressure this process of discharge restarting is more important than the photoelectric one; on the contrary, the contribution of the Penning effect is of the same order of the photoelectric effect at 1000 mm Hg pressure.

The pulse shapes at the corona threshold shown in Fig. 19 are in accord with this description of the mechanism controlling the corona discharge, due to the fact that the continuous slope of the pulses indicates a process of electron production in the gas.

Argon plus 0.1 percent carbon dioxide plus mercury vapor mixtures have also been studied. In this case the counter behaves as if filled with argon plus 0.1 percent carbon dioxide only. We observe that in these mixtures the quenching effect of carbon dioxide will reduce the lifetime of excited levels in the gas and consequently will reduce the collision probability on mercury atoms until the mercury ionization becomes negligible.

[25] Processes of this kind may be caused by the argon atoms excited in the upper levels (~15 ev), which may produce electrons by means of a reaction, for instance,

$$A^*+A\rightarrow(A_2)^*\rightarrow A_2^+ + e^-,$$

recently studied by Molnar and Hornbeck [J. A. Hornbeck, Phys. Rev. 84, 615 (1951); J. A. Hornbeck and J. P. Molnar, Phys. Rev. 84, 621 (1951)], or by means of ionizing collisions on atoms or molecules of a suitable gas. Under these conditions, the discharge spreading may be favored by the diffusion of the excited atoms in a small zone surrounding the wire, due to the imprisonment effect suffered by the resonance photons emitted by the highly excited atoms.

[26] D. Willard and C. G. Montgomery, Rev. Sci. Instr. **21**, 52 (1950).

X. CONCLUSION

In those mixtures where the photoelectric effect is the main process acting in the discharge build-up, the contribution to the pulse formation caused by the Townsend avalanche can be separated from the contribution caused by secondary processes. Consequently, it is possible to study the secondary process of electron production and measure its efficiency.

From our results the photoelectric process on the cathode is found to be responsible for the formation of the Geiger and corona zones in mixtures of argon plus carbon dioxide at concentrations less than 5×10^{-3} at any pressure used.

The same accuracy cannot be used in the study of mixtures where a process of electron production in the gas body will operate, as in the case of argon plus carbon dioxide, at percentage higher than 5×10^{-3}. However, these processes are very interesting due to their fast spreading.

Furthermore, the photons acting in the photoelectric effect on the cathode are found to be emitted by the first excited levels of argon. These photons are produced in collisions leading to destruction of these levels, and are not resonance photons. The values obtained for the lifetimes of these levels are roughly in accordance with the extrapolation of Molnar's values at the pressure used. More direct measurement of these lifetimes at pressures ranging from 10 to 1000 mm should be very interesting in order to investigate this effect further.

We wish to take this opportunity to thank Professor G. Bolla and Professor B. Ferretti for assistance received during this work, Dr. F. M. Penning for his interest and valuable discussions, Dr. Molnar and Dr. Hornbeck for notifying us of their results, and Dr. E. Gatti for helpful discussions. We finally wish to thank Professor L. Loeb for his interesting critique and for the useful suggestions offered to us.

PHYSICAL REVIEW VOLUME 88, NUMBER 5 DECEMBER 1, 1952

Range Distribution of Sea-Level Mesons at Low Geomagnetic Latitudes*

L. DEL ROSARIO AND J. DÁVILA-APONTE
Physics Department, University of Puerto Rico, Rio Piedras, Puerto Rico
(Received July 31, 1952)

Seven points of the meson differential spectrum at sea level have been obtained at a geomagnetic latitude of 29°N. The method used was that of delayed coincidences and anticoincidences, and the range interval covered has been from about 10 to 320 g/cm² of air equivalent. In this interval our spectrum curve is found to be nearly flat; that is, it does not show a clear maximum around 200 g/cm² air equivalent, as indicated by several authors working at geomagnetic latitudes around 45°N.

I. INTRODUCTION

THE range and the momentum distribution of sea-level ordinary mesons (μ-mesons) have been investigated in the past years by several authors[1] working at geomagnetic latitudes around 45°N. Various techniques have been employed for this purpose: coincidence, anticoincidence, delayed coincidence, and magnetic deflection methods.

Although it is quite well known that only a very small percentage of the charged particles at sea level are protons, as yet little information is available on the energy distribution of these protons. For this reason, and also in order to get rid of the electronic component, without uncertainty, even at very low energies the method of delayed coincidences (which yields the complete separation of the mesons at rest taking advantage of their instability) appears to be the most suitable to investigate the low energy end of the meson spectrum. This technique has also the advantage of being much simpler and less expensive than the one based on the use of a Wilson chamber in a magnetic field. It cannot be profitably used, however, for an accurate determination of the absolute number of the observed mesons, since it is in general difficult to evaluate the efficiency of the apparatus for the detection of the electrons resulting from the decay of the stopped mesons.

To overcome this point, delayed coincidences and anticoincidences have been recorded simultaneously in

* This investigation was sponsored jointly by the ONR and by a grant-in-aid from the Research Corporation.

[1] M. H. Shamos and M. G. Levy, Phys. Rev. **73**, 1396 (1948); A. Rogozinski and M. Lesage, Compt. rend. **227**, 1027 (1948); B. G. Owen and J. G. Wilson, Proc. Phys. Soc. (London) **62**, 600 (1949); E. W. Kellerman and K. Westerman, Proc. Phys. Soc. (London) **A62**, 356 (1949); W. L. Kraushaar, Phys. Rev. **76**, 1045 (1949); M. Sands, Phys. Rev. **77**, 180 (1950); M. Conversi, Phys. Rev. **79**, 749 (1950); L. Germain, Phys. Rev. **80**, 616 (1950); Glaser, Hamermesh, and Safonov, Phys. Rev. **80**, 625 (1950); Caro, Parry, and Rathgeber, Nature **165**, 688 (1950); M. G. Mylroi and J. G. Wilson, Proc. Phys. Soc. (London) **A64**, 404 (1951); B. G. Owen and J. G. Wilson, Proc. Phys. Soc. (London) **A64**, 417 (1951); J. L. Zar, Phys. Rev. **83**, 761 (1951); C. M. York, Phys. Rev. **85**, 998 (1952). For work previous to 1948, see B. Rossi, Revs. Modern Phys. **20**, 537 (1948); articles by G. Puppi and N. Dallaporta and by George in *Progress in Cosmic Ray Physics* (North-Holland Publishing Company, Amsterdam, 1952). An investigation on the spectrum of high range mesons has been recently published by Brini, Rimondi, and Filosofo, Nuovo cimento **9**, 505 (1952).

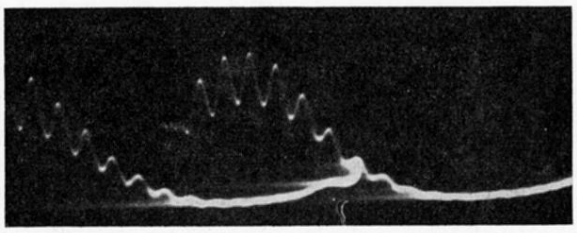

FIG. 11. β-pulses in the Geiger zone. Argon plus $\sim 10^{-3}$ carbon dioxide; pressure = 760 mm Hg; sweep time = 50 μsec; $RC = 1$ μsec.

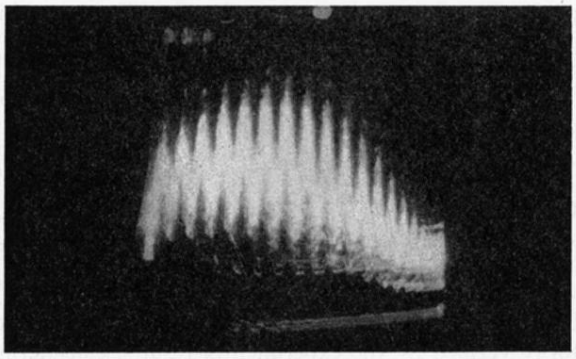

FIG. 12. Several superposed β-pulses in the Geiger zone. Argon plus 1.7 10^{-3} carbon dioxide; pressure = 1000 mm Hg; distance between photopulses = 4.4 μsec; $RC = 1$ μsec.

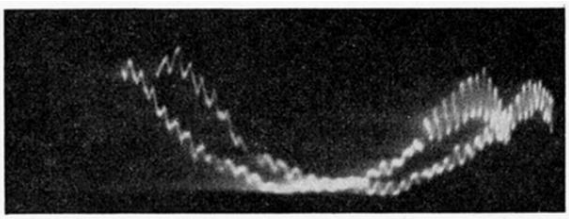

FIG. 13. Detailed bursts in unstable corona zone. Argon plus $\sim 10^{-3}$ carbon dioxide; pressure = 760 mm Hg; sweep time = 100 μsec; $RC = 1$ μsec.

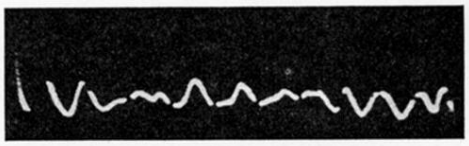

FIG. 14. Burst at the end of unstable corona zone. Argon plus $\sim 10^{-3}$ carbon dioxide; counter diameter = 20 mm; pressure = 760 mm Hg; markers = 100 μsec; $RC = 10$ μsec; The photoelectric pulse groups appear like single pulses, due to the high RC value.

FIG. 15. Bursts in unstable corona zone. Argon plus $\sim 10^{-3}$ carbon dioxide; counter diameter = 130 mm; pressure = 760 mm Hg; sweep time = 30 msec; $RC = 200$ μsec.

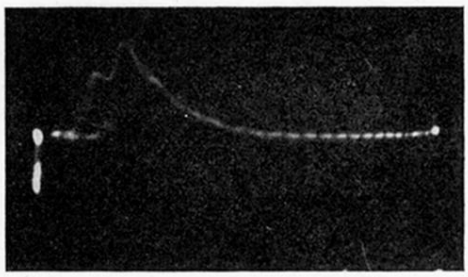

FIG. 16. Geiger pulse in the middle Geiger zone. Argon plus 10^{-2} carbon dioxide; pressure = 500 mm Hg; markers = 1 μsec; $RC = 1$ μsec. The discharge spreading is due to both the photoelectric effect and a production of electrons in the gas.

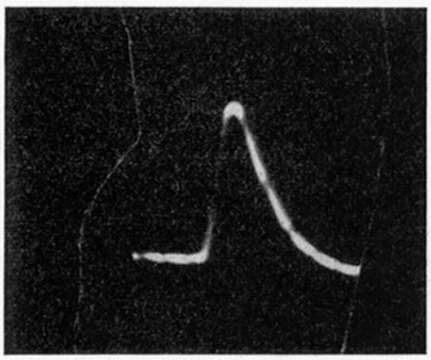

FIG. 17. Several superposed fast pulses at the end of the Geiger zone. Argon plus 10^{-2} carbon dioxide; pressure = 500 mm Hg; markers = 1 μsec; $RC = 1$ μsec. The discharge will spread solely by the process producing electrons in the gas body.

FIG. 19. α-particle pulses in argon plus mercury vapor at the corona threshold. Pressure = 1000 mm Hg; markers = 1 μsec; $RC = 1$ μsec. The slow decay is due to production of electrons in the gas.

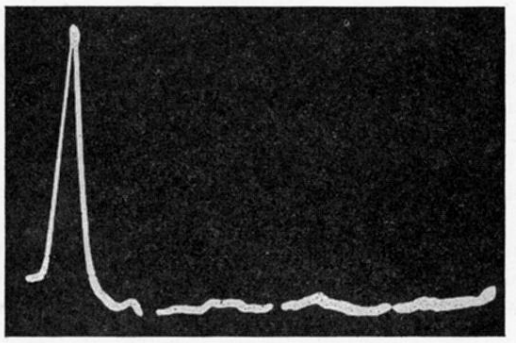

FIG. 3. α-particle pulse in the low proportional zone. Markers = 10 μsec; $RC = 1$ μsec.

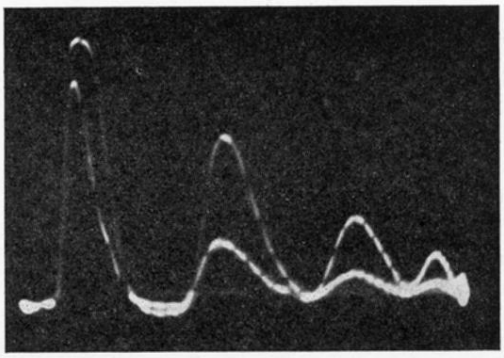

FIG. 4. α-particle pulses in argon at the corona threshold. Pressure $=1000$ mm Hg; $N=210$; markers $=1$ μsec; $RC=1$ μsec.

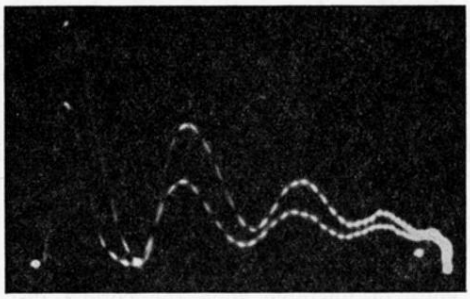

FIG. 5. α-particle pulses in argon at the corona threshold. Pressure = 500 mm Hg; $N = 250$; lengthening of rise time is detectable in the last photopulses; markers = 1 μsec; $RC = 1$ μsec.

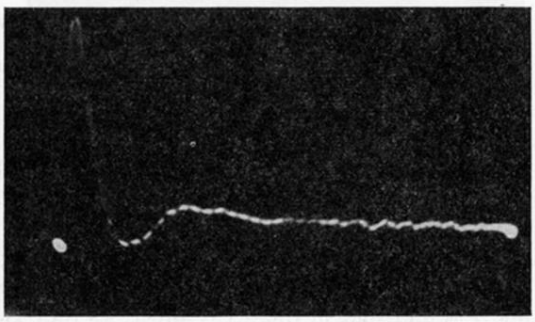

FIG. 6. α-particle pulse in argon at the corona threshold. Pressure $=150$ mm Hg; $N=180$; markers $=1$ μsec; $RC=1$ μsec.

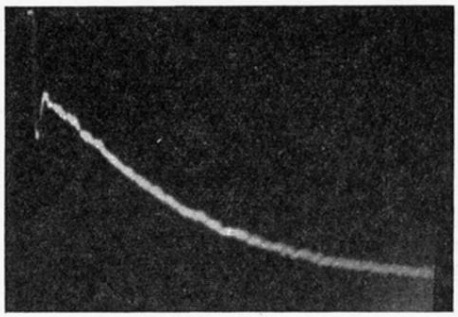

FIG. 7. α-particle pulse in argon at the corona threshold. Pressure = 150 mm Hg; $N = 180$; sweep time = 100 μsec; $RC = 10$ μsec.

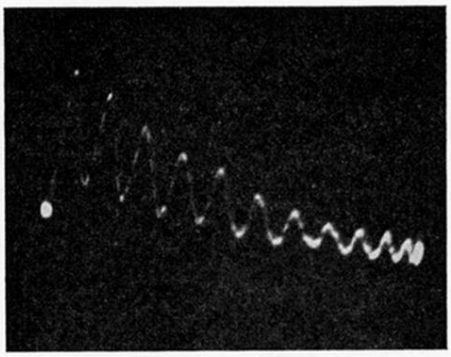

FIG. 8. β-pulse in argon plus 5×10^{-4} carbon dioxide near the Geiger threshold. Pressure = 500 mm Hg; markers = 1 μsec; $RC = 1$ μsec.

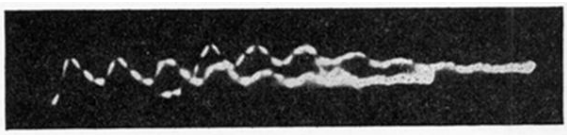

FIG. 9. β-pulses in argon plus 17×10^{-4} carbon dioxide around the Geiger threshold. Pressure=150 mm Hg; markers=1 μsec; RC=1 μsec.